Investigation of Effect of Creep Strain on Low-Cycle Fatigue of Lead-Free Solder by Cyclic Loading Using Stepped Ramp Waves

Ken-ichi Ohguchi[1]
Department of Materials Science and Engineering,
Akita University,
Tegatagakuen-cho 1-1,
Akita 010-8502, Japan
e-mail: ken@ipc.akita-u.ac.jp

Katsuhiko Sasaki
Division of Human Mechanical Systems and Design,
Hokkaido University,
N13, W8, Kita-ku,
Sapporo 060-8628, Japan

The fatigue life of a material varies with the strain rate if it has time-dependent deformation. An interesting phenomenon related to the effect of the strain rate on the fatigue life can be observed when a cyclic tension-compression loading of which strain rate in the tensile region is different from that in the compressive region is employed for the fatigue test. Different fatigue lives due to different strain rates in the tensile and compression regions originate from the difference of development behaviors of creep strain generated in the cyclic loading. This paper investigates the effects of creep strain on the difference of fatigue life due to the different strain rate in the tensile and compression regions. The creep strain of the lead-free solder Sn–3.0Ag–0.5Cu subjected to a cyclic loading was investigated using stepped ramp wave loading. The experimental results reveal that the creep strain develops differently in the tensile and compression regions. A new parameter is proposed for estimating fatigue life when the strain rate varies in the loading direction. [DOI: 10.1115/1.4002911]

Keywords: lead-free solder, low-cycle fatigue, strain rate effect, creep strain, stress relaxation, cyclic loading

1 Introduction

Solder joints are subjected to cyclic inelastic deformation due to electronic parts having different coefficients of thermal expansion. Since cyclic deformation causes low-cycle fatigue failure of solder joints, many researchers have experimentally investigated the fatigue strength of solder alloys [1–8]. In addition, many researchers have investigated the fatigue strength of solder joints by combining experimental methods using simulated solder joint specimens with finite element analysis (FEA) [9–13]. The strain rate affects the fatigue life of solder alloys because solder alloys exhibit remarkable time-dependent deformation [3,14–16]. An interesting phenomenon related to the effect of the strain rate on the fatigue life can be observed when a cyclic tension-compression loading of which strain rate in the tensile region is different from that in the compressive region is employed for the fatigue test. Therefore, a few studies have investigated the fatigue behaviors of solder alloys subjected to cyclic tension-compression loading for the case when there are different strain rates in the tensile and compression regions [6–8].

Tokimasa [6] conducted fatigue tests using 63Sn–37Pb solders for several loading conditions having triangular strain waveforms for which the following combinations of ramp up and ramp down rates were used: fast-fast, fast-slow, slow-fast, and slow-slow. The fatigue lives were analyzed by the creep-fatigue damage rule. Zhang et al. [7] also conducted fatigue tests using Sn–3.0Ag–0.5Cu lead-free solder for several loading conditions by employing fast-fast, fast-slow, slow-fast, and strain-hold strain waveforms; they also proposed a method for predicting creep-fatigue life. Both of these studies found that the slow-fast condition (for which the strain rate on the tensile side is lower than that on the compression side) gives the shortest fatigue life of all the test conditions. This is related to creep strain generated during cyclic loading because creep strain increases as the strain rate decreases. Then, the fatigue life may decrease when creep strain increases in the tensile region.

Kariya et al. [8] conducted fatigue tests using miniature specimens of Sn–3.0Ag–0.5Cu and Sn–37Pb solders and for fast-fast and slow-fast loading conditions. They found that the inelastic strain amplitude was strongly correlated with the fatigue life. However, they showed that the correlation varied depending on the loading conditions. The fatigue lives for the slow-fast and fast-fast loading conditions differed greatly, despite the two loading conditions having almost equal inelastic strain amplitudes. This phenomenon was also observed by Zhang et al. [7]. Thus, the inelastic strain amplitude is not the best parameter for precisely predicting the fatigue lives of solders that are affected by the strain rate and an alternative parameter is required. Based on the above discussion, the creep strain is a key factor for predicting the fatigue lives of solders that are affected by the strain rate.

We have proposed methods for determining the creep strain in both lead and lead-free solders for pure tension and cyclic tension-compression loading [17–19]. These methods can successfully evaluate the creep strain without conducting creep tests, and they also quantify the creep strain during loading (e.g., for pure tension and cyclic loading). In particular, we quantified the creep strain in tensile and cyclic tension-compression loading by a method that employed stepped ramp wave (SW) loading [20,21].

In the present study, this method was applied to cyclic tension-compression loading for fatigue tests of Sn–3.0Ag–0.5Cu lead-free solder. The cyclic loading employed different periods on the tensile and compressive regions. Using the creep strain determined by the above method that employs SW loading, we proposed an effective parameter for predicting fatigue lives that de-

[1]Corresponding author.

Contributed by the Electronic and Photonic Packaging Division of ASME for publication in the JOURNAL OF ELECTRONIC PACKAGING. Manuscript received December 13, 2009; final manuscript received September 14, 2010; published online December 3, 2010. Assoc. Editor: Bongtae Han.

Table 1 Test conditions for fatigue tests

Number	Strain amplitude $\Delta\varepsilon$ (%)	Time period T/s		Temperature
1	±0.5	T_t (tensile side)	2	Room temperature (RT, 295 K)
		T_c (compressive side)	20	
2	±0.5	T_t (tensile side)	20	
		T_c (compressive side)	2	
3	±0.5	T_t (tensile side)	2	
		T_c (compressive side)	200	
4	±0.5	T_t (tensile side)	200	
		T_c (compressive side)	2	

pend on the strain rate. To investigate and discuss the above-mentioned things, fatigue tests were conducted first using a triangular wave (TW) for loading, which is generally used for fatigue tests. Then, to analyze the creep strains generated in the fatigue tests using TW loading, fatigue tests for SW loading were conducted using the same strain amplitude and time period as those for the fatigue test using TW loading. Using the stress-strain relations obtained by SW loading, the creep strains generated in the fatigue tests using TW loading were identified. Finally, based on these creep strains, a method for predicting the fatigue life of solders affected by the strain rate is discussed.

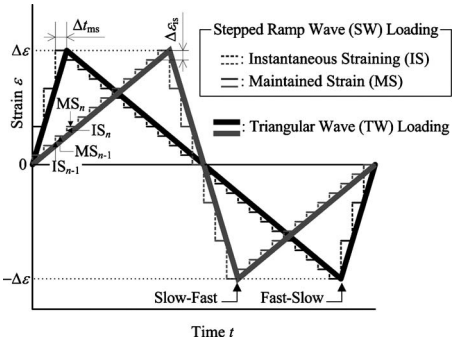

Fig. 1 Schematic outline of the waveforms used for cyclic tension-compression loading

2 Experimental Procedures

The fatigue test specimens were made of the lead-free solder alloy Sn–3.0Ag–0.5Cu. Cylindrical ingots of the solder alloy were machined into specimens. The specimens have a gauge length of 18 mm and a gauge diameter of 8 mm [20,21]. Based on the test standard by the Society of Materials Science, Japan (JSMS) [22], the specimens were annealed at $0.87T_m$ (where T_m is the melting temperature in kelvin) for 1 h after machining.

Fatigue tests were conducted with cyclic tension-compression loadings with different periods on the tensile and compression sides (see Table 1) for a total strain amplitude of ±0.5% at 295 K. First, the fatigue tests employed TW loadings to clarify the effect of the difference of the period on fatigue lives. These cyclic tension-compression loadings were applied after first applying TW loading. Second, to identify creep deformation strain generated during the fatigue tests by cyclic TW loadings, fatigue tests employing cyclic SW loadings were also conducted after TW loading. Figure 1 shows a schematic outline of the waveforms used for cyclic tension-compression loading. The SW loading consists of an instantaneous straining (IS) part and a maintained strain (MS) part (see Fig. 1). These two components were stepped repeatedly. The subscript n of IS and MS in Fig. 1 denotes the number of repeated steps during SW loading. The strain is maintained for a period Δt_{ms} for MS loading, and the strain increases due to instantaneous loading until $\Delta\varepsilon_{is}$ for IS loading. In this study, Δt_{ms} was chosen to be 0.5 s for all the test conditions given in Table 1 because we had previously quantified the creep strains

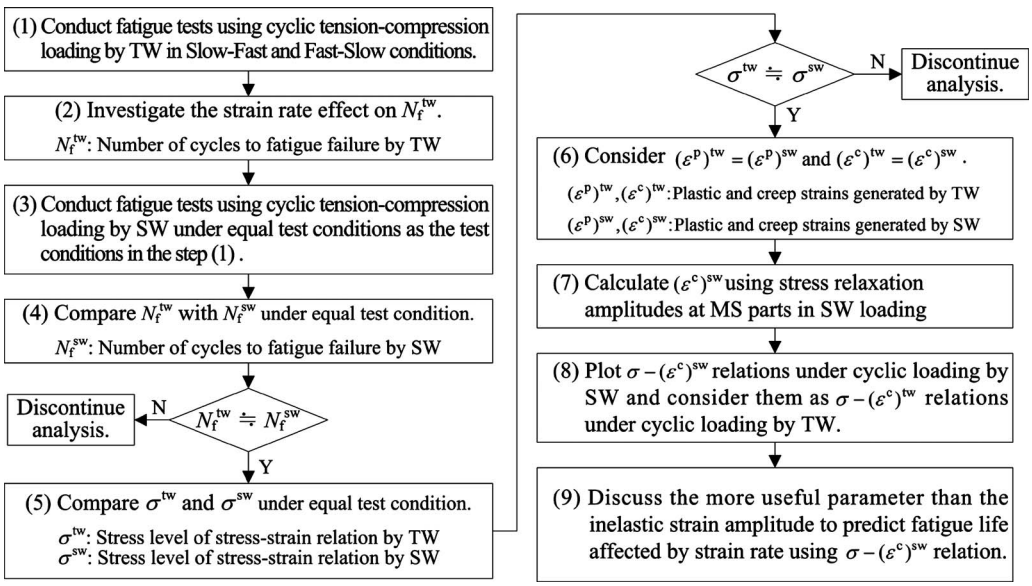

Fig. 2 Road map for experimental procedure

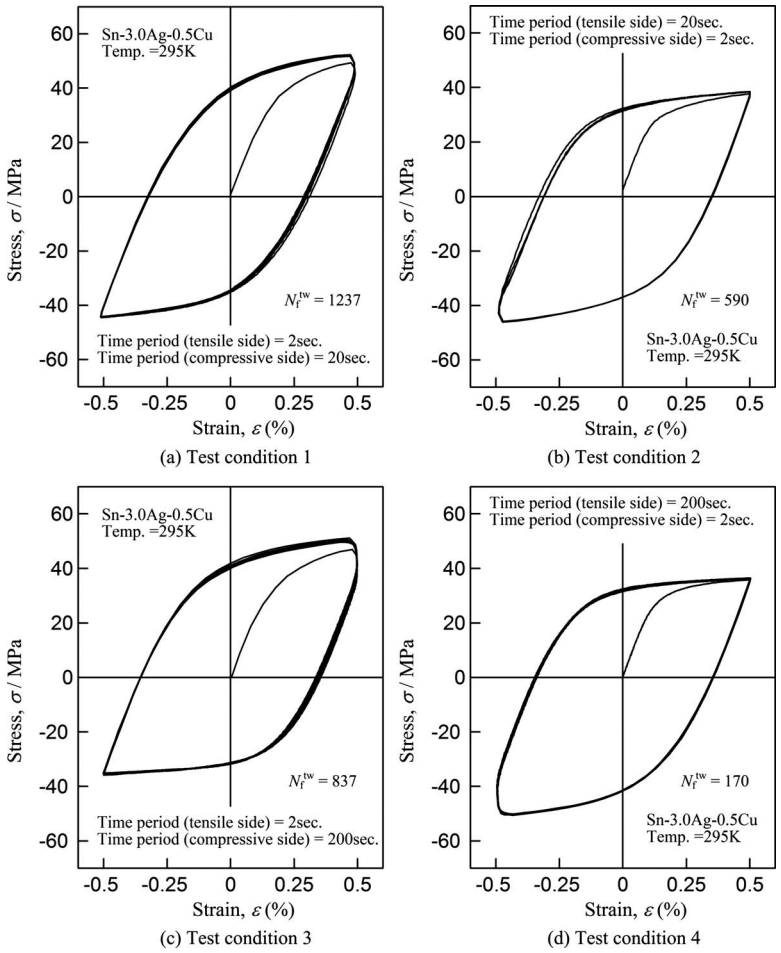

Fig. 3 Hysteresis loops for TW loading: test conditions (*a*) 1, (*b*) 2, (*c*) 3, and (*d*) 4

generated in cyclic loading using a Δt_{ms} of 0.5 s [21]. The testing machine for all the tests was a Servopulser EHF-FB1 (Shimadzu Co., Ltd., Japan). The strain and stress measurement precisions are 1.0×10^{-3}% and 1.9×10^{-2} MPa, respectively.

Figure 2 shows the road map for the experimental procedure. Fatigue tests using cyclic tension-compression TW loading for slow-fast and fast-slow conditions were first conducted (step (1)). After conducting these tests, we investigated the effect of the strain rate on the number of cycles to fatigue failure for TW loading (N_f^{tw}) (step (2)). Next, fatigue tests were performed using cyclic tension-compression SW loading for the same test conditions as those used in step (1) (step (3)). The number of cycles to fatigue failure for SW loading (N_f^{sw}) was compared with N_f^{tw}, and the stress level of the stress-strain relation for TW loading (σ^{tw}) was compared with that for SW loading (σ^{sw}) (steps (4) and (5)). When the fatigue lives N_f and the stress levels for the same test conditions became equal for the TW and SW loadings, we considered that the plastic and creep strains generated by the two loadings were equal (step (6)). Based on this, the creep strains generated by the cyclic loadings were quantified (steps (7) and (8)). Finally, based on the quantified creep strains, we discuss a more useful parameter than the inelastic strain amplitude for predicting fatigue lives that are affected by the strain rate (step (9)).

3 Experimental Results

Figures 3(*a*)–3(*d*) show the stress-strain relations for five cycles of TW loading for test conditions 1–4, respectively. The stress-strain relations in Fig. 3 stabilized within a few loading cycles for all four test conditions. The stress-strain relations in Fig. 3 are asymmetric with respect to the origin because of the different loading periods on the tensile and compressive sides. The hysteresis loops are truncated at points where the strain rate changes from being high to low. These are caused by stress relaxation that occurs for sudden reductions in the strain rate.

For the fast-slow cases for test conditions 1 and 3, the maximum absolute stress on the tensile side is higher than that on the compressive side, whereas for the slow-fast cases for test conditions 2 and 4, the maximum absolute stress on the compressive side is higher than that on the tensile side. The larger difference in the period results in larger differences in the maximum absolute stress. Therefore, the stress-strain relations for test conditions 3 and 4 exhibit remarkable asymmetry.

The numbers for N_f^{tw} shown in Figs. 3(*a*)–3(*d*) are the number of cycles to fatigue failure. The number of cycles to fatigue failure for slow-fast loading is fewer than that for fast-slow loading. This suggests that it is possible for the numbers of cycles to fatigue failure to be different even when the periods in one loading cycle are the same. Since slow loading generates a larger creep strain than fast loading, the difference in the number of cycles to fatigue failure is caused by differences in the generated creep strains for the four test conditions. The fatigue life is expected to decrease when the creep strain generated on the tensile side of cyclic loading increases.

Figure 4 shows the relationship between the inelastic strain amplitude $\Delta\varepsilon^{in}$ and N_f^{tw}. The inelastic strain amplitudes $\Delta\varepsilon^{in}$ shown in Fig. 4 were obtained from the strain difference between two points with zero stress in the hysteresis loop of the fifth cycle. The

No.	$\Delta\varepsilon$ (%)	T (sec.)		N_f^{tw} (cycles)	Temp.
1	±0.5	T_t	2	1237	RT (295K)
		T_c	20		
2	±0.5	T_t	20	590	
		T_c	2		
3	±0.5	T_t	2	837	
		T_c	200		
4	±0.5	T_t	200	170	
		T_c	2		

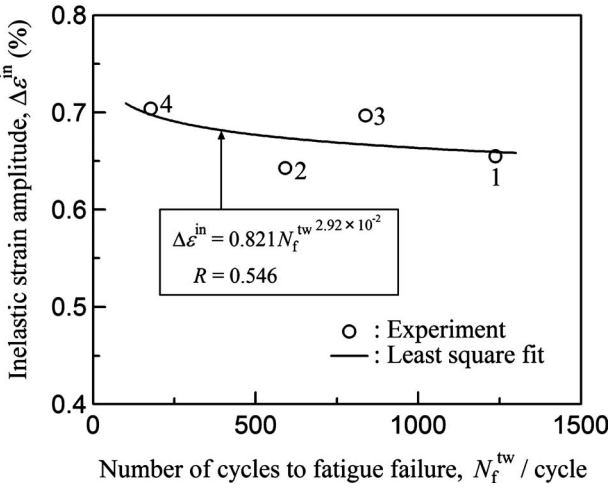

Fig. 4 Relationship between inelastic strain amplitude and fatigue life N_f^{tw} for TW loading

numbers in Fig. 4 indicate the test condition numbers given in Table 1. The values of N_f^{tw} for each test condition are listed above the figure. The inelastic strain amplitudes for test conditions 1 and 2 are almost the same; in addition, the inelastic strain amplitudes for test conditions 3 and 4 are almost the same. The inelastic strain amplitudes $\Delta\varepsilon^{in}$ are the same when the periods for a loading cycle are the same. However, the numbers of cycles to fatigue failure N_f^{tw} are very different despite the inelastic strain amplitudes $\Delta\varepsilon^{in}$ being the same. This phenomenon was also observed by Zhang et al. [7].

The solid line in Fig. 4 shows the relationship between the $\Delta\varepsilon^{in}$ and the N_f^{tw} approximated by a power law. This approximation is unacceptable because its correlation factor R is low, being 0.546. This means that the inelastic strain amplitude $\Delta\varepsilon^{in}$ cannot be used to estimate fatigue failure due to cyclic tension-compression loading with different strain rates on the tensile and compressive sides. Since N_f^{tw} is affected by creep deformation, a parameter for estimating fatigue failure should consider creep deformation during cyclic deformation. Therefore, the behavior of creep strain during cyclic deformation should be clarified.

4 Method for Identifying Creep Strain During Cyclic Loading

4.1 Stress-Strain Relation and Fatigue Life for SW Loading. To identify the development behaviors of creep strain generated by cyclic TW loading, we have previously proposed a method that employed SW loading [21]. In the method, fatigue lives for TW loading were compared with those for SW in same test condition that has the same periods on the tensile and compression sides. As a result of comparison, the fatigue lives were almost equal between TW and SW in the same test condition. This revealed that the creep strains generated during TW and SW loadings were the same because the IS and the MS did not affect the number of cycles to fatigue failure if the test conditions for the TW and SW loadings were the same [21].

In the present study, stress-strain relations and fatigue lives for SW loading for the four test conditions given in Table 1 were investigated to compare those for TW loading. If the stress-strain relations and fatigue lives for SW are almost equal to those for TW loadings in each test condition, the creep strain for SW loading can be regarded as the creep strain for TW loading for the four test conditions [21].

Figures 5(*a*)–5(*d*) show the stress-strain relations for up to five cycles of SW loading for test conditions 1–4, respectively. They show that the stress fluctuates due to IS and MS in SW loading. The maximum absolute stress values on the tensile and compression sides of SW loading are almost the same as those for TW loading shown in Fig. 3; i.e., the deviations in the maximum absolute stresses on the tensile and compression sides are almost the same.

Figure 6 compares the fatigue lives for SW and TW loadings for the same loading conditions. In Fig. 6, N_f^{sw} is the fatigue life for SW loading and N_f^{tw} is the fatigue life for TW loading. The open circles show the results obtained in the present study, and the open squares indicate the results obtained in a previous study [21] for which the periods for loading are the same on the tensile and compression sides. Figure 6 reveals that the number of cycles to fatigue failure caused by SW loading is almost the same as that for TW loading, despite the loadings having different periods on the tensile and compression sides. These results suggest that the plastic and creep strains generated by SW loading should equal those generated by TW loading [21]. The following analysis of the creep strain was conducted based on this assumption.

4.2 Creep Strain Analysis. The so-called elastic-plastic-creep model is regarded as the most suitable constitutive model for solders, and it is widely used in FEA of solder joints. In this model, the total strain $\boldsymbol{\varepsilon}$ consists of three strains: elastic, plastic, and creep strains; i.e.,

$$\boldsymbol{\varepsilon} = \boldsymbol{\varepsilon}^e + \boldsymbol{\varepsilon}^p + \boldsymbol{\varepsilon}^c \tag{1}$$

where $\boldsymbol{\varepsilon}^e$ and $\boldsymbol{\varepsilon}^p$ are, respectively, the time-independent elastic and plastic strains and $\boldsymbol{\varepsilon}^c$ is the time-dependent creep strain.

The elastic strain $\boldsymbol{\varepsilon}^e$ can be expressed by Hooke's law:

$$\boldsymbol{\varepsilon}^e = (\boldsymbol{D}^e)^{-1}:\boldsymbol{\sigma} \tag{2}$$

where $\boldsymbol{\sigma}$ is the Cauchy stress tensor and $\boldsymbol{D}^e$ is the elastic tensor.

To incorporate the constitutive model into FEA, the plastic strain $\boldsymbol{\varepsilon}^p$ is often expressed in the following discrete form using the backward Euler method:

$$\boldsymbol{\varepsilon}^p_{i+1} = \boldsymbol{\varepsilon}^p_i + \Delta\boldsymbol{\varepsilon}^p \tag{3}$$

where the subscripts i and $i+1$, respectively, denote the start and end of a calculation step and $\Delta\boldsymbol{\varepsilon}^p$ is the plastic strain increment in the current calculation step. The creep strain $\boldsymbol{\varepsilon}^c$ is expressed in the following discrete form:

$$\boldsymbol{\varepsilon}^c_{i+1} = \boldsymbol{\varepsilon}^c_i + \Delta\boldsymbol{\varepsilon}^c \tag{4}$$

Like the plastic and creep strains, the elastic strain shown in Eq. (2) can be rewritten in the following discrete form:

$$\boldsymbol{\varepsilon}^e_{i+1} = \boldsymbol{\varepsilon}^e_i + \Delta\boldsymbol{\varepsilon}^e = \boldsymbol{\varepsilon}^e_i + (\boldsymbol{D}^e)^{-1}:\Delta\boldsymbol{\sigma} \tag{5}$$

The total strain increment can then be expressed as

$$\Delta\boldsymbol{\varepsilon} = \Delta\boldsymbol{\varepsilon}^e + \Delta\boldsymbol{\varepsilon}^p + \Delta\boldsymbol{\varepsilon}^c \tag{6}$$

Figure 7 shows an enlargement of a part of the first quadrant of Fig. 5(*d*) that clearly indicates stress fluctuations due to SW loading. The stress reductions caused by the MS for a time of Δt_{ms} are known as stress relaxation amplitudes $\Delta\sigma_t$ and are shown in Fig. 7. Since the total strain increments are equal to zero and plastic strain is not generated in the MS regions, $\Delta\boldsymbol{\varepsilon}$ and $\Delta\boldsymbol{\varepsilon}^p$ in Eq. (6) can be set to zero [20,21]. Therefore, the stress relaxation amplitude $\Delta\sigma_t$ can be expressed as

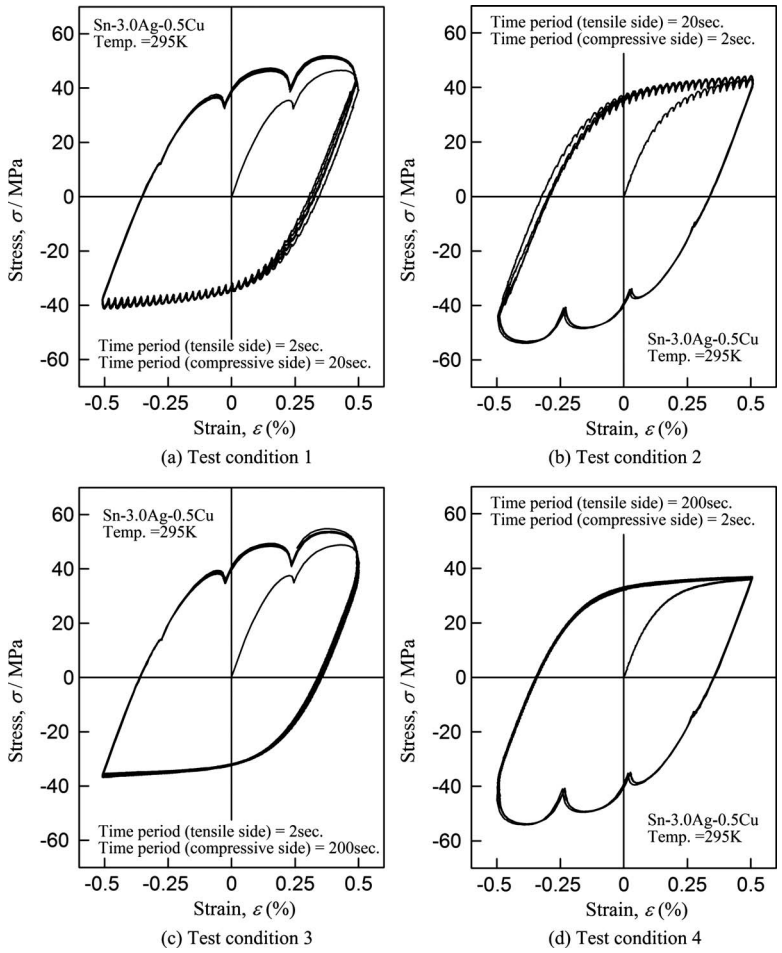

Fig. 5 Hysteresis loops for SW loading. Test conditions (*a*) 1, (*b*) 2, (*c*) 3, and (*d*) 4

$$\Delta\varepsilon_t^c = -\Delta\sigma_t/E \tag{7}$$

where E is the Young's modulus and the subscript t denotes the uniaxial condition. In this study, the Young's modulus E was set to 26.0 GPa. This value was obtained from the stress-strain relation in four stresses in the range 0–15 MPa; the effect of creep deformation on the stress-strain relation is very small in this range.

Assuming that the creep strain is not generated in the IS regions, it is possible to quantify the creep strain that is generated in SW loading by summing the creep strain increments $\Delta\varepsilon_t^c$ calculated by Eq. (7) in each MS region. The quantified creep strain for SW loading is considered as the creep strain during TW loading because the creep strains generated during TW and SW loadings are almost equal for the same loading conditions. Consequently,

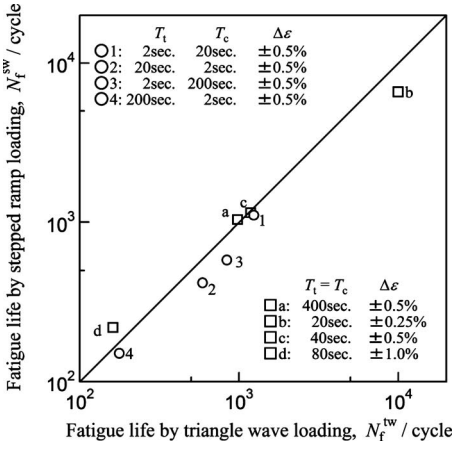

Fig. 6 Comparison between N_f^{sw} for SW loading and N_f^{tw} for TW loading

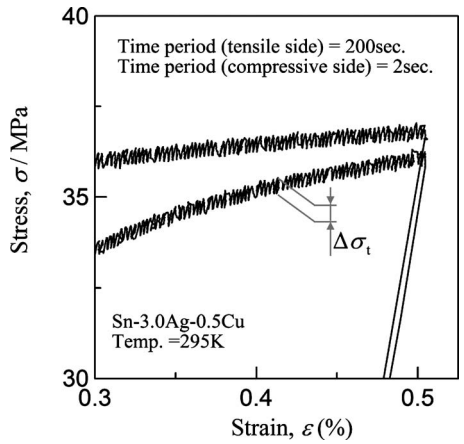

Fig. 7 Enlargement of the first quadrant of Fig. 5(*d*)

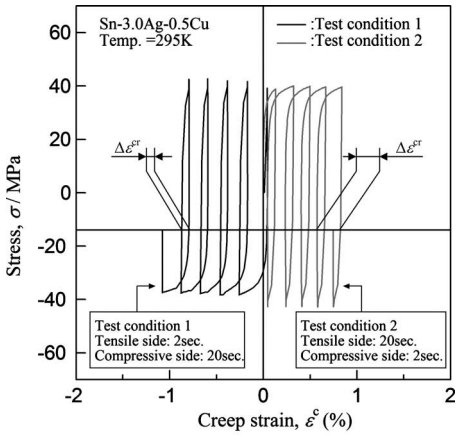

(a) Test conditions 1 and 2

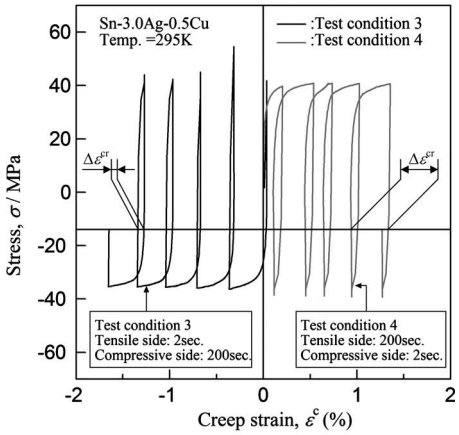

(b) Test conditions 3 and 4

Fig. 8 Comparison of relationship between stress and creep strain: test conditions (*a*) 1 and 2 and (*b*) 3 and 4

the creep strains in the stress-strain relations shown in Figs. 3(*a*)–3(*d*) were quantified based on the method.

5 Results and Discussion

Figure 8 shows the relationships between the stress and creep strain for the four test conditions. Figure 8(*a*) shows the results for test conditions 1 and 2, and Fig. 8(*b*) shows those for test conditions 3 and 4. The creep strain accumulates in the compressive direction for the fast-slow condition for test conditions 1 and 3, whereas it accumulates in the tensile direction for the slow-fast condition for test conditions 2 and 4.

The number of cycles to fatigue failure for the slow-fast condition is lower than for the fast-slow condition, as shown in Fig. 3. This is because the creep strain that accumulates in the tensile direction (see Fig. 8) greatly affects the fatigue life; greater accumulation of tensile creep strain reduces the fatigue life. This implies that the creep strain generated on the tensile side of cyclic loading is closely correlated with the fatigue lives. Thus, a parameter that considers creep strain should be employed to accurately evaluate the fatigue life. Therefore, the relationship between the creep strain amplitudes $\Delta\varepsilon^{cr}$ on the tensile side of cyclic tension-compression loading and the number of cycles to fatigue failure is discussed. The creep strain amplitude $\Delta\varepsilon^{cr}$ for each cyclic loading was obtained from the stress-creep strain relation in the fifth cycle, as shown in Fig. 8.

Figure 9 shows the relationship between the creep strain amplitude $\Delta\varepsilon^{cr}$ and the number of cycles to fatigue failure for TW loading. The solid line in Fig. 9 shows an approximation curve based on the following power law:

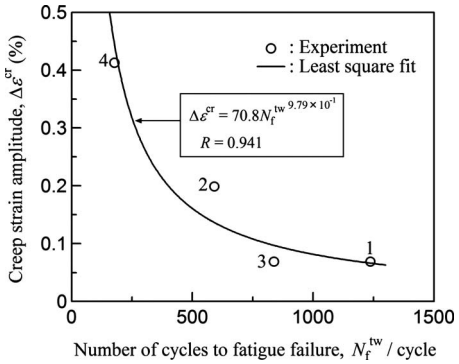

Fig. 9 Relationship between creep strain amplitude $\Delta\varepsilon^{c}$ and fatigue life N_f^{tw} for TW loading

$$\Delta\varepsilon^{cr} = 70.8(N_f^{tw})^{9.79\times10^{-1}} \tag{8}$$

Since the correlation factor R for the approximation expressed by Eq. (8) has a high value of 0.941 (see Fig. 9), the approximation curve expresses well the relationship between $\Delta\varepsilon^{cr}$ and N_f^{tw}. Because the inelastic strain amplitude $\Delta\varepsilon^{in}$ is not well correlated with N_f^{tw} (see Fig. 4), it is preferable to use the creep strain amplitude $\Delta\varepsilon^{cr}$ defined in Fig. 8 as a parameter for evaluating the fatigue life.

6 Conclusions

This paper considered the fatigue lives of Sn–3.0Ag–0.5Cu lead-free solder for cyclic tension-compression loading in which the periods on the tensile and compression sides are different. In addition, to determine an effective parameter for predicting the fatigue life, a method that identifies the creep strain generated in cyclic loading was proposed by employing SW loading. The following conclusions were obtained:

(1) The fatigue life of the lead-free solder Sn–3.0Ag–0.5Cu subjected to cyclic tension-compression loading with a slow-fast TW was shorter than that subjected to cyclic fast-slow TW loading. In addition, the fatigue life for slow-fast TW loading decreased with a reduction in the strain rate on the tensile side.
(2) The number of cycles to fatigue failure for SW loadings, which includes repeated cycles of IS and MS, were almost the same as those for TW loadings. Therefore, there is assumed to be little difference in the basic deformation for TW and SW loadings.
(3) Based on the assumption in (2), the creep strain for cyclic tension-compression loading was identified by applying a numerical method for determining the stress relaxation curves obtained for the MS regions in SW loading.
(4) The creep strain for slow-fast cyclic loading accumulates in the tensile direction, whereas that for fast-slow loading accumulates in the compression direction, and the accumulated creep strain increases with increasing loading period.
(5) The creep strain accumulated on the tensile side greatly affects the fatigue life. Therefore, the creep strain amplitude $\Delta\varepsilon^{cr}$ was determined using the stress-creep strain relation on the tensile side in the fifth cycle. The creep strain amplitude $\Delta\varepsilon^{cr}$ has a higher correlation factor with fatigue life than the inelastic strain amplitude $\Delta\varepsilon^{in}$. The applicability of $\Delta\varepsilon^{cr}$ for estimating the fatigue life due to thermal fatigue of a solder needs to be considered.

Acknowledgment

This study was supported by a Grant-in-Aid for Scientific Research (C) from the Japan Society for the Promotion of Science (Grant No. 19560071).

Nomenclature

$\Delta\varepsilon_{is}$ = strain increment for instantaneous straining
Δt_{ms} = time for maintaining strain
$\boldsymbol{\varepsilon}$ = total strain in the elastic-plastic-creep model
$\boldsymbol{\varepsilon}^e, \boldsymbol{\varepsilon}^p, \boldsymbol{\varepsilon}^c$ = elastic, plastic, and creep strains, respectively
$\boldsymbol{\sigma}$ = stress
$\boldsymbol{D}^e$ = elastic tensor
$\Delta\boldsymbol{\sigma}$ = stress increment
$\Delta\boldsymbol{\varepsilon}$ = total strain increment
$\Delta\boldsymbol{\varepsilon}^e$ = elastic strain increment
$\Delta\boldsymbol{\varepsilon}^p$ = plastic strain increment
$\Delta\boldsymbol{\varepsilon}^c$ = creep strain increment
$\Delta\varepsilon_t^c$ = uniaxial creep strain increment
$\Delta\sigma_t$ = stress relaxation amplitude
E = Young's modulus
$\Delta\varepsilon^{in}$ = inelastic strain amplitude
N_f^{tw} = number of cycles to fatigue failure by triangular wave loading
N_f^{sw} = number of cycles to fatigue failure by stepped ramp wave loading
$\Delta\varepsilon^{cr}$ = creep strain amplitude

References

[1] Solomon, H. D., and Tolksdorf, E. D., 1995, "Energy Approach to the Fatigue of 60/40 Solder: Part I—Influence of Temperature and Cycle Frequency," ASME J. Electron. Packag., **117**, pp. 130–135.
[2] Leece, G. D., Miskioglu, I., and Nelson, D. A., 1996, "Experimental Investigation of the Effects of Cycling Frequency and Temperature on the Fatigue Life of 60 Tin/40 Lead Solder," ASME J. Electron. Packag., **118**, pp. 280–284.
[3] Ishikawa, H., Sasaki, K., and Ohguchi, K., 1996, "Prediction of Fatigue Failure of 60Sn–40Pb Solder Using Constitutive Model for Cyclic Viscoplasticity," ASME J. Electron. Packag., **118**, pp. 164–169.
[4] Wen, S., and Keer, L. M., 2002, "A Theory of Fatigue: A Physical Approach With Application to Lead-Rich Solder," ASME J. Appl. Mech., **69**, pp. 1–10.
[5] Liang, J., Dariavach, N., Callahan, P., and Shangguan, D., 2007, "Inelastic Deformation and Fatigue of Solder Alloys Under Complicated Load Conditions," ASME J. Electron. Packag., **129**, pp. 195–204.
[6] Tokimasa, K., 2004, "Creep-Fatigue Properties of Sn-37Pb Solder Material Evaluated by Room Temperature Testing Under Various Strain Waveforms," JSME Int. J., Ser. A, **47**, pp. 380–388.
[7] Zhang, S., Ogawa, S., and Sakane, M., 2009, "Creep-Fatigue Life Assessment for Sn-3.0Ag-0.5Cu Solder," Journal of Solid Mechanics and Materials Engineering, **3**, pp. 507–517.
[8] Kariya, Y., Niimi, T., Suga, T. and Otsuka, M., 2005, "Low Cycle Fatigue Properties of Solder Alloys Evaluated by MICRO Bulk Specimen," Proceedings of IPACK2005, IPACK Paper No. 2005-73165.
[9] Roellig, M., Dudek, R., Wiese, S., Boehme, B., Wunderle, B., Wolter, K. J., and Michel, B., 2007, "Fatigue Analysis of Miniaturized Lead-Free Solder Contacts Based on a Novel Test Concept," Microelectron. Reliab., **47**, pp. 187–195.
[10] Erinc, M., Schreurs, P. J. G., and Geers, M. G. D., 2007, "Integrated Numerical–Experimental Analysis of Interfacial Fatigue Fracture in SnAgCu Solder Joints," Int. J. Solids Struct., **44**, pp. 5680–5694.
[11] Ladani, L. J., and Razmi, J., 2009, "An Anisotropic Mechanical Fatigue Damage Evolution Model for Pb-Free Solder Materials," Mech. Mater., **41**, pp. 878–885.
[12] Herkommer, D., Punch, J., and Reid, M., 2010, "A Reliability Model for SAC Solder Covering Isothermal Mechanical Cycling and Thermal Cycling Conditions," Microelectron. Reliab., **50**, pp. 116–126.
[13] Kuna, M., and Wippler, S., 2010, "A Cyclic Viscoplastic and Creep Damage Model for Lead Free Solder Alloys," Eng. Fract. Mech., in press.
[14] Nose, H., Sakane, M., Tsukada, Y., and Nishimura, H., 2003, "Temperature and Strain Rate Effects on Tensile Strength and Inelastic Constitutive Relationship of Sn-Pb Solders," ASME J. Electron. Packag., **125**, pp. 59–66.
[15] Ohguchi, K., and Sasaki, K., 2001, "Description of Temperature Dependence and Creep Deformation of 60Sn–40Pb Solder Alloys," JSME Int. J., Ser. A, **44**, pp. 82–88.
[16] Sasaki, K., Ohguchi, K., and Ishikawa, H., 2001, "Viscoplastic Deformation of 40Pb/60Sn Solder Alloys—Experiments and Constitutive Modeling," ASME J. Electron. Packag., **123**, pp. 379–387.
[17] Ohguchi, K., and Sasaki, K., 2003, "Elastic-Plastic-Creep Simulation of Pb/Sn Solder Alloys by Separation of Plastic and Creep," JSME Int. J., Ser. A, **46**, pp. 559–566.
[18] Ohguchi, K., Sasaki, K., Ishibashi, M., and Hoshino, T., 2004, "Plasticity-Creep Separation Method for Viscoplastic Deformation of Lead-Free Solders," JSME Int. J., Ser. A, **47**, pp. 371–379.
[19] Ohguchi, K., Sasaki, K., and Ishibashi, M., 2006, "A Quantitative Evaluation of Time-Independent and Time-Dependent Deformations of Lead-Free and Lead-Containing Solder Alloys," J. Electron. Mater., **35**, pp. 132–139.
[20] Ohguchi, K., Sasaki, K., and Aso, S., 2009, "Evaluation of Time-Independent and Time-Dependent Strains of Lead-Free Solder by Stepped Ramp Loading Test," ASME J. Electron. Packag., **131**, p. 021003.
[21] Ohguchi, K., and Sasaki, K., 2010, "Time-Independent and Time-Dependent Inelastic Strains Analysis of Lead-Free Solder by Cyclic Stepped Ramp Wave Loading Test," ASME J. Electron. Packag., **132**, p. 041003.
[22] The Society of Materials Science, Japan, 2001, "Factual Database on Tensile and Low Cycle Fatigue Properties of Sn-37Pb and Sn-3.5Ag Solders," The Society of Materials Science, Japan, p. 102.